Complete hyperentangled state analysis and generation of multi-particle entanglement based on charge detection*

Ji Yan-Qiang(计彦强)[a], Jin Zhao(金 钊)[a], Zhu Ai-Dong(朱爱东)[a]†, Wang Hong-Fu(王洪福)[a,b], and Zhang Shou(张 寿)[a]

[a] *Department of Physics, College of Science, Yanbian University, Yanji* 133002, *China*
[b] *School of Physics and Optoelectronic Technology, Dalian University of Technology, Dalian* 116024, *China*

(Received 9 August 2013; revised manuscript received 10 September 2013; published online 25 March 2014)

We propose the schemes for implementing hyperentangled state analysis and generating four-electron high entangled states (including cluster state, $|\chi\rangle$ state, and symmetric Dicke state) based on the charge detection of free electrons. These schemes are deterministic and rely only on charge detection and single-spin rotations. This method, which uses noninteracting electrons, is not only efficient but also saves on quantum resources.

Keywords: hyperentanglement analysis, charge detection, noninteracting electrons

PACS: 03.67.–a, 03.67.Hk, 42.50.Ex **DOI:** 10.1088/1674-1056/23/5/050306

1. Introduction

Entanglement plays an important role in quantum information processing (QIP). It has been widely used in quantum teleportation,[1] quantum cryptographic schemes,[2,3] quantum secret sharing,[4–7] quantum key distribution,[8–11] and quantum secure direct communication.[12–21] Moreover, the multi-particle entangled states, e.g., cluster state,[22–27] $|\chi\rangle$ state,[28] and symmetric Dicke state,[29] occupy an important position in one-way quantum computation due to their high entanglements.[30] Hyperentanglement is the simultaneous entanglement in more than one degree of freedom, such as polarization–momentum, polarization–spatial, spatial–spin, and so on. It provides an effective and practical capacity-increased way to manipulate qubits in QIP in comparison with the normal entanglement and is widely used in Bell-state analysis,[31–36] entanglement purification,[37–43] and quantum repeaters.[44] Kwiat and Weinfurter demonstrated that a complete Bell-state analysis can be achieved with additional degrees of freedom, such as time and momentum.[31] Walborn *et al*. proposed a linear optical scheme for Bell-state measurement by using hyperentangled states in 2003.[32] Sheng *et al*. proposed a scheme for implementing a complete hyperentangled-Bell-state analysis (HBSA) in the polarization and spatial-mode degrees of freedom with the help of cross-Kerr nonlinearity.[33] Ren *et al*. also proposed an HBSA scheme with a photon system assisted by quantum dot spins in optical microcavities.[34]

The charge detector is a powerful instrument and plays a key role in the QIP of free electrons, which can be realized by using a point contact made of a quantum dot with a resonant conductance.[45] Free-electron quantum computation can be accomplished by encoding quantum information in the spin degree of freedom of the conduction electrons. Similar to photons, electrons can also act as flying qubits. Since Beenakker *et al*. constructed a deterministic CNOT gate between flying electronic qubits based on charge detection and showed that QIP with electrons could be simpler than that with photons,[46] charge detection has drawn much attention. For example, in 2005, Feng *et al*. proposed an entanglement purification scheme for the mixed entangled states of electrons with the aid of charge detection.[47] Sheng *et al*. proposed an entanglement concentration protocol for electrons based on their spins and charge,[48] later, they implemented a multi-particle entanglement purification scheme.[49] Wang *et al*. implemented the fermionic quantum swap and Fredkin gates for spin qubits based on charge detection.[50] Zhou implemented an entanglement concentration for the electron-spin W state with charge detection.[51]

In this paper, we implement an HBSA based on charge detection. This HBSA scheme can be divided into two steps. The first step is used to distinguish the Bell state in the spatial-mode degree of freedom, and the second step is used to distinguish the Bell state in the spin degree of freedom. Subsequently, we suggest schemes for generating the multi-particle entangled states, including four-electron cluster state, $|\chi\rangle$ state, and symmetric Dicke state based on charge detection. Comparing with the other schemes, our scheme does not require an auxiliary system, and only relies on charge detection and single-spin rotations.

The remainder of the paper is organized as follows. In Section 2, a scheme is proposed for deterministically distin-

*Project supported by the National Natural Science Foundation of China (Grant Nos. 11165015, 61068001, and 11264042) and the Natural Science Foundation of Jilin Province, China (Grant No. 201115226).

†Corresponding author. E-mail: adzhu@ybu.edu.cn

© 2014 Chinese Physical Society and IOP Publishing Ltd

guishing a hyperentangled Bell state in the electron spin degree of freedom and the spatial modes. In Section 3, we propose schemes for generating a four-electron cluster state, a $|\chi\rangle$ state, and a symmetric Dicke state. Finally, a discussion and a summary are given in Section 4.

2. HBSA in spatial mode and electron spin degree of freedom

A two-path parity meter for electron spatial mode is introduced, which is composed of two charge detectors and two electronic polarizing beam splitters (PBS), as shown in Fig. 1. The $P_{\rm u}$ and $P_{\rm d}$ are normal charge detectors used to distinguish the occupation states of the upper and the lower paths, respectively. They can distinguish the occupation number 1 from 0 or 2 in a nondestructive way, but cannot distinguish between 0 and 2. The PBS is a polarizing beam splitter which transmits the electrons with spin up and reflects those with spin down. The parity P of the two spatial modes is determined by the measurement results of $P_{\rm u}$ and $P_{\rm d}$ according to the following relation: $P=1$ for $\{P_{\rm u}=0,P_{\rm d}=1\}$ or $\{P_{\rm u}=1,P_{\rm d}=0\}$, and $P=0$ for $\{P_{\rm u}=0,P_{\rm d}=0\}$ or $\{P_{\rm u}=1,P_{\rm d}=1\}$. Two electrons in an arbitrary spin Bell state passing through this parity meter will not be changed in path and spin. When the two electrons are input from the upper and the lower paths, respectively (this situation corresponds to $P=0$), their parity of spin can be identified. Namely, the result $P_{\rm u}=P_{\rm d}=1$ implies two identical spins ($\uparrow\uparrow$ or $\downarrow\downarrow$), while $P_{\rm u}=P_{\rm d}=0$ implies two different spins ($\uparrow\downarrow$ or $\downarrow\uparrow$). If only one path has an input electron ($P=1$), the result $\{P_{\rm u}=0,P_{\rm d}=1\}$ implies a spin up (down) input from the upper (lower) path, and $\{P_{\rm u}=1,P_{\rm d}=0\}$ implies a spin up (down) input from the lower (upper) path. These features can be applied to entangled state analysis.

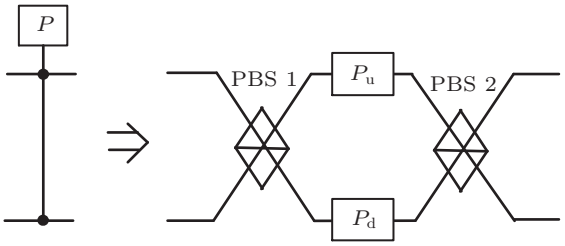


Fig. 1. A two-path parity meter P for electronic spatial mode consists of two normal charge detectors ($P_{\rm u}$ and $P_{\rm d}$) and two PBSs which transmit spin-up electrons and reflect spin-down ones.

The schematic diagram of the HBSA is shown in Fig. 2, where P_1 and P_2 are two two-path parity meters, P_3 and P_4 are two normal charge detectors, the BS is a 50 : 50 beam splitter, and the PBS is a polarizing beam splitter which transmits spin-up electrons and reflects spin-down ones.

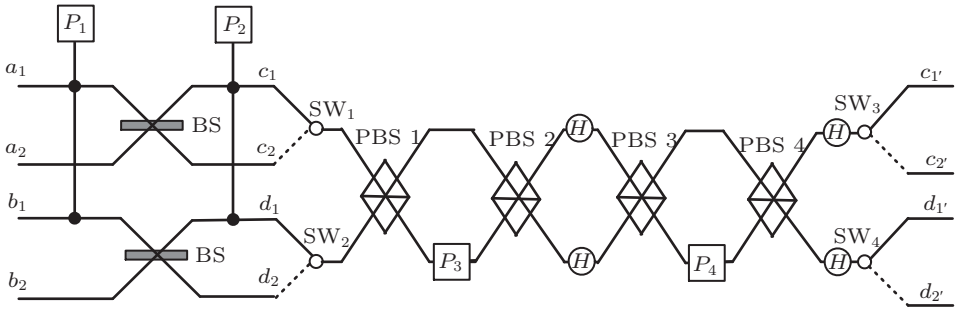


Fig. 2. Schematic diagram of the HBSA. The BS is a 50 : 50 beam splitter, P_1 and P_2 are two two-path parity meters, and P_3 and P_4 are two normal charge detectors. The SW is a switch controlling the path of a electron, SW_1 and SW_3 should be switched simultaneously to the upper or lower path to keep entanglement in the spatial-mode degree of freedom, and SW_2 and SW_4 should also be switched simultaneously.

The initial state of two electrons entangled simultaneously in spatial-mode and spin degrees of freedom can be expressed as

$$|\varphi\rangle = |i\rangle_1 \otimes |i\rangle_2, \tag{1}$$

where i=$\{\Phi^{\pm},\Psi^{\pm}\}$, subscripts 1 and 2 represent spatial-mode and spin degrees of freedom, respectively. We denote the four Bell states in the spatial-mode degree of freedom as

$$\begin{aligned} |\Phi^{\pm}\rangle_1 &= \frac{1}{\sqrt{2}}(|a_1b_1\rangle \pm |a_2b_2\rangle), \\ |\Psi^{\pm}\rangle_1 &= \frac{1}{\sqrt{2}}(|a_1b_2\rangle \pm |a_2b_1\rangle), \end{aligned} \tag{2}$$

and the four Bell states in the spin degree of freedom as

$$\begin{aligned} |\Phi^{\pm}\rangle_2 &= \frac{1}{\sqrt{2}}(|\uparrow\uparrow\rangle \pm |\downarrow\downarrow\rangle), \\ |\Psi^{\pm}\rangle_2 &= \frac{1}{\sqrt{2}}(|\uparrow\downarrow\rangle \pm |\downarrow\uparrow\rangle), \end{aligned} \tag{3}$$

where a_1 (a_2) and b_1 (b_2) are different spatial modes, and $|\uparrow\rangle$ and $|\downarrow\rangle$ denote spin up and spin down of the electrons, respectively. We can distinguish states $|\Phi^{\pm}\rangle_1$ from $|\Psi^{\pm}\rangle_1$ by using P_1. Then the two electrons pass through two 50 : 50 BSs, respectively, which accomplish the following transformation in

the spatial modes

$$
\begin{aligned}
|a_1\rangle &\to \frac{1}{\sqrt{2}}(|c_1\rangle + |c_2\rangle),\\
|a_2\rangle &\to \frac{1}{\sqrt{2}}(|c_1\rangle - |c_2\rangle),\\
|b_1\rangle &\to \frac{1}{\sqrt{2}}(|d_1\rangle + |d_2\rangle),\\
|b_2\rangle &\to \frac{1}{\sqrt{2}}(|d_1\rangle - |d_2\rangle).
\end{aligned} \tag{4}
$$

Then equation (2) evolves as

$$
\begin{aligned}
|\Phi^+\rangle_1 &= \frac{1}{\sqrt{2}}(|c_1d_1\rangle + |c_2d_2\rangle),\\
|\Phi^-\rangle_1 &= \frac{1}{\sqrt{2}}(|c_1d_2\rangle + |c_2d_1\rangle),\\
|\Psi^+\rangle_1 &= \frac{1}{\sqrt{2}}(|c_1d_1\rangle - |c_2d_2\rangle),\\
|\Psi^-\rangle_1 &= \frac{1}{\sqrt{2}}(|c_2d_1\rangle - |c_1d_2\rangle).
\end{aligned} \tag{5}
$$

By using P_2, we can distinguish state $|\Phi^+\rangle_1$ from $|\Phi^-\rangle_1$ and state $|\Psi^+\rangle_1$ from $|\Psi^-\rangle_1$.

Table 1. Measurement results and the corresponding Bell states.

P_1	P_2	P_3	P_4	Initial Bell state
0	0	0	0	$\|\Phi^+\rangle_1 \otimes \|\Psi^-\rangle_2$
0	0	0	1	$\|\Phi^+\rangle_1 \otimes \|\Psi^+\rangle_2$
0	0	1	0	$\|\Phi^+\rangle_1 \otimes \|\Phi^-\rangle_2$
0	1	0	0	$\|\Phi^-\rangle_1 \otimes \|\Psi^-\rangle_2$
1	0	0	0	$\|\Psi^+\rangle_1 \otimes \|\Psi^-\rangle_2$
0	0	1	1	$\|\Phi^+\rangle_1 \otimes \|\Phi^+\rangle_2$
0	1	1	0	$\|\Phi^-\rangle_1 \otimes \|\Phi^-\rangle_2$
1	1	0	0	$\|\Psi^-\rangle_1 \otimes \|\Psi^-\rangle_2$
0	1	0	1	$\|\Phi^-\rangle_1 \otimes \|\Psi^+\rangle_2$
1	0	1	0	$\|\Psi^+\rangle_1 \otimes \|\Phi^-\rangle_2$
1	0	0	1	$\|\Psi^+\rangle_1 \otimes \|\Psi^+\rangle_2$
0	1	1	1	$\|\Phi^-\rangle_1 \otimes \|\Phi^+\rangle_2$
1	1	1	0	$\|\Psi^-\rangle_1 \otimes \|\Phi^-\rangle_2$
1	1	0	1	$\|\Psi^-\rangle_1 \otimes \|\Psi^+\rangle_2$
1	0	1	1	$\|\Psi^+\rangle_1 \otimes \|\Phi^+\rangle_2$
1	1	1	1	$\|\Psi^-\rangle_1 \otimes \|\Phi^+\rangle_2$

The method to distinguish the four Bell states $|\Phi^\pm\rangle_2$ and $|\Psi^\pm\rangle_2$ in the spin degree of freedom is similar to that in Ref. [22]. As shown in Fig. 2, the two Hadamard operations are used to recover the initial Bell state in spin, and $H = (\sigma_x + \sigma_z)/\sqrt{2}$, whose actions are given by $\{|\uparrow\rangle \to (|\uparrow\rangle + |\downarrow\rangle)/\sqrt{2}, |\downarrow\rangle \to (|\uparrow\rangle - |\downarrow\rangle)/\sqrt{2}\}$. The switches are used to control the paths of the electrons. It is necessary to switch SW_1 and SW_3 simultaneously to the upper paths c_1 and $c_{1'}$ or the lower paths c_2 and $c_{2'}$ to keep the entanglement in the spatial-mode degree of freedom. In the same way, SW_2 and SW_4 should also be switched simultaneously to paths d_1 and $d_{1'}$ or d_2 and $d_{2'}$. For example, if we obtain the Bell state $|\Phi^+\rangle_1 = (|c_1d_1\rangle + |c_2d_2\rangle)/\sqrt{2}$ according to P_1 and P_2, we need to switch SW_1 and SW_2 simultaneously to paths c_1 and d_1, SW_3 and SW_4 simultaneously to paths $c_{1'}$ and $d_{1'}$, after that, switch SW_1 and SW_2 to paths c_2 and d_2, and SW_3 and SW_4 to paths $c_{2'}$ and $d_{2'}$. We can properly adjust the path lengths of c_2, d_2, $c_{1'}$, and $d_{1'}$ to make the electrons reach the output at the same time. The corresponding measurement results are shown in Table 1. By this means, all of the hyperentangled Bell states can be distinguished and the initial hyperentangled state is not destroyed.

3. Generation of multi-particle entanglement states

3.1. Four-electron cluster state

The cluster state is a type of high entangled state of multi-particle, which has special applications in measurement-based quantum computation. Now we propose a scheme to generate a four-electron cluster state using PBS_i $(i = 1,2,\ldots,6)$, charge detectors P_i $(i = 1,2,3)$, and Hadamard transformation. The schematic diagram of our scheme is shown in Fig. 3.

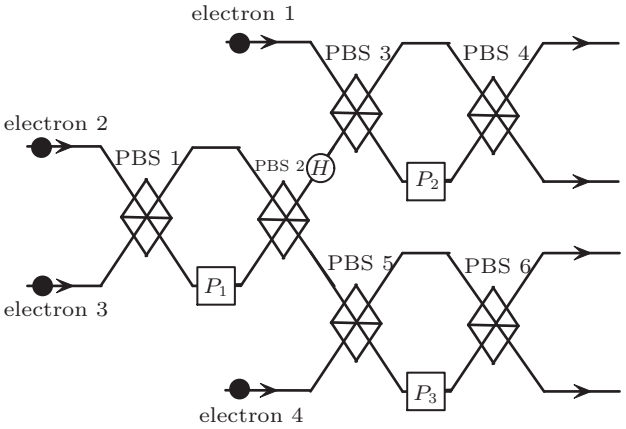


Fig. 3. The schematic diagram of cluster state preparation. The PBS_i $(i = 1,2,\ldots,6)$ are polarizing beam splitters which transmit spin-up electrons and reflect spin-down ones, P_i $(i = 1,2,3)$ are the charge detectors, and H is the Hadamard transformation.

We assume that all of the electrons are in state $|\varphi\rangle_i = (|\uparrow\rangle + |\downarrow\rangle)/\sqrt{2}$, $(i = 1,2,3,4)$. So the input state of the whole system is

$$
|\psi\rangle_0 = |\varphi\rangle_1 \otimes |\varphi\rangle_2 \otimes |\varphi\rangle_3 \otimes |\varphi\rangle_4. \tag{6}
$$

After a series of setups shown in Fig. 3, the charge detectors P_i $(i = 1,2,3)$ record the electronic bunching $(P_i = 0)$ or antibunching $(P_i = 1)$, then a four-electron cluster state can be obtained in a deterministic fashion by applying a local single-qubit spin rotation to the qubits according to the measurement results of the charge detectors. For example, if $P_1 = P_2 = 1$ and $P_3 = 0$, the evolution can be written as follows:

$$
\frac{1}{4}(|\uparrow\rangle + |\downarrow\rangle)(|\uparrow\rangle + |\downarrow\rangle)(|\uparrow\rangle + |\downarrow\rangle)(|\uparrow\rangle + |\downarrow\rangle)
$$

$$\begin{aligned}
&\xrightarrow{P_1=1} \frac{1}{2\sqrt{2}}(|\uparrow\rangle+|\downarrow\rangle)(|\uparrow\uparrow\rangle+|\downarrow\downarrow\rangle)(|\uparrow\rangle+|\downarrow\rangle)\\
&\xrightarrow{H} \frac{1}{4}(|\uparrow\rangle+|\downarrow\rangle)(|\uparrow\uparrow\rangle+|\downarrow\uparrow\rangle+|\uparrow\downarrow\rangle-|\downarrow\downarrow\rangle)(|\uparrow\rangle+|\downarrow\rangle)\\
&\xrightarrow{P_2=1} \frac{1}{2\sqrt{2}}(|\uparrow\uparrow\uparrow\rangle+|\downarrow\downarrow\uparrow\rangle+|\uparrow\uparrow\downarrow\rangle-|\downarrow\downarrow\downarrow\rangle)(|\uparrow\rangle+|\downarrow\rangle)\\
&\xrightarrow{P_3=0} \frac{1}{2}(|\uparrow\uparrow\uparrow\downarrow\rangle+|\downarrow\downarrow\uparrow\downarrow\rangle+|\uparrow\uparrow\downarrow\uparrow\rangle-|\downarrow\downarrow\downarrow\uparrow\rangle)\\
&\xrightarrow{\sigma_x^4} |\text{cluster state}\rangle. \qquad (7)
\end{aligned}$$

Table 2. The obtained output states and the single-qubit local rotation operations required for achieving the four-electron cluster states corresponding to different measurement values of charge detectors P_1, P_2, and P_3. Here σ_x^j are Pauli operators on the spin qubit, and I is the identity operator.

P_1	P_2	P_3	Output state	Operations
1	1	1	$\frac{1}{2}(\lvert\uparrow\uparrow\uparrow\uparrow\rangle+\lvert\uparrow\uparrow\downarrow\downarrow\rangle+\lvert\downarrow\downarrow\uparrow\uparrow\rangle-\lvert\downarrow\downarrow\downarrow\downarrow\rangle)$	I
1	0	0	$\frac{1}{2}(\lvert\downarrow\uparrow\uparrow\downarrow\rangle+\lvert\downarrow\uparrow\downarrow\uparrow\rangle+\lvert\uparrow\downarrow\uparrow\downarrow\rangle-\lvert\uparrow\downarrow\downarrow\uparrow\rangle)$	$\sigma_x^1\otimes\sigma_x^4$
1	1	0	$\frac{1}{2}(\lvert\uparrow\uparrow\uparrow\downarrow\rangle+\lvert\uparrow\uparrow\downarrow\uparrow\rangle+\lvert\downarrow\downarrow\uparrow\downarrow\rangle-\lvert\downarrow\downarrow\downarrow\uparrow\rangle)$	σ_x^4
1	0	1	$\frac{1}{2}(\lvert\downarrow\uparrow\uparrow\uparrow\rangle+\lvert\downarrow\uparrow\downarrow\downarrow\rangle+\lvert\uparrow\downarrow\uparrow\uparrow\rangle-\lvert\uparrow\downarrow\downarrow\downarrow\rangle)$	σ_x^1
0	1	1	$\frac{1}{2}(\lvert\uparrow\uparrow\downarrow\downarrow\rangle+\lvert\uparrow\uparrow\uparrow\uparrow\rangle+\lvert\downarrow\downarrow\downarrow\downarrow\rangle-\lvert\downarrow\downarrow\uparrow\uparrow\rangle)$	$\sigma_x^3\otimes\sigma_x^4$
0	0	0	$\frac{1}{2}(\lvert\downarrow\uparrow\downarrow\uparrow\rangle+\lvert\downarrow\uparrow\uparrow\downarrow\rangle+\lvert\uparrow\downarrow\uparrow\downarrow\rangle-\lvert\uparrow\downarrow\uparrow\uparrow\rangle)$	$\sigma_x^1\otimes\sigma_x^3$
0	1	0	$\frac{1}{2}(\lvert\uparrow\uparrow\downarrow\uparrow\rangle+\lvert\uparrow\uparrow\uparrow\downarrow\rangle+\lvert\downarrow\downarrow\downarrow\uparrow\rangle-\lvert\downarrow\downarrow\uparrow\downarrow\rangle)$	σ_x^3
0	0	1	$\frac{1}{2}(\lvert\downarrow\uparrow\downarrow\downarrow\rangle+\lvert\downarrow\uparrow\uparrow\uparrow\rangle+\lvert\uparrow\downarrow\downarrow\downarrow\rangle-\lvert\uparrow\downarrow\uparrow\uparrow\rangle)$	$\sigma_x^1\otimes\sigma_x^3\otimes\sigma_x^4$

The other measurement results and the corresponding local single-qubit spin rotations are listed in Table 2. Note that Zhang *et al*. and Tang also proposed some schemes for preparing the cluster state by using parity and controlled-phase gates,[22,23] and Ionicioiu implemented cluster state fusion deterministically with parity measurements.[52] Compared to those schemes, the present one is simpler due to there being no requirement for ancilla.

3.2. Four-electron $|\chi\rangle$ state

A four-electron $|\chi\rangle$ state is written as

$$\begin{aligned}
|\chi\rangle = \frac{1}{2}[&(|\uparrow\rangle|\uparrow\rangle+|\downarrow\rangle|\downarrow\rangle)|\uparrow\rangle|\uparrow\rangle\\
&+(|\uparrow\rangle|\downarrow\rangle+|\downarrow\rangle|\uparrow\rangle)|\downarrow\rangle|\downarrow\rangle]. \qquad (8)
\end{aligned}$$

This state has been proved to be optimal, violated a new Bell inequality, and has been used to carry out quantum communication,[53] so it is very important for QIP. The schematic diagram for preparing the $|\chi\rangle$ state is shown in Fig. 4, which includes the PBSs, charge detectors P_i $(i=1,2,3)$, and Hadamard operations.

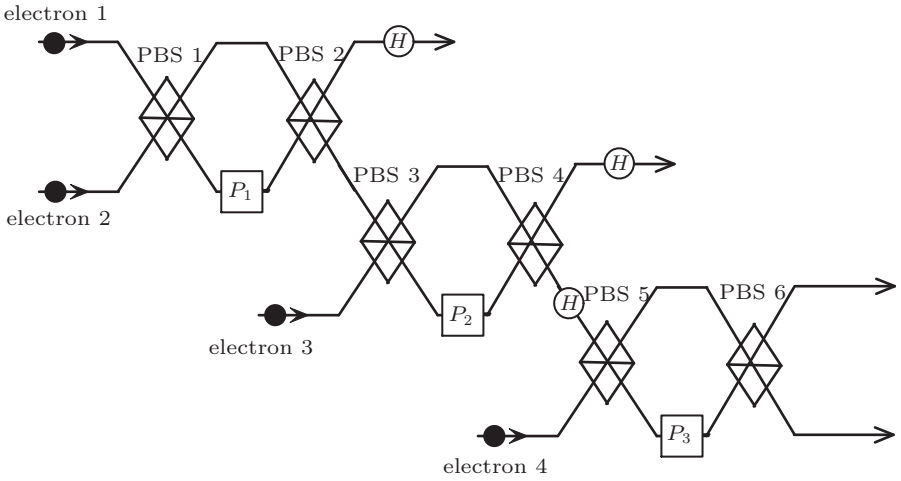


Fig. 4. The schematic diagram of $|\chi\rangle$ state preparation.

Initially, all of the four electrons are in the state $(|\uparrow\rangle+|\downarrow\rangle)/\sqrt{2}$. After a series of setups shown in Fig. 4, according to the measurement results of the charge detectors, a four-electron $|\chi\rangle$ state can be obtained in a deterministic fashion by applying local single-qubit spin rotation operations. For example, for $P_1=P_2=1$ and $P_3=0$, the evolution can be written as follows:

$$\begin{aligned}
&\frac{1}{4}(|\uparrow\rangle+|\downarrow\rangle)(|\uparrow\rangle+|\downarrow\rangle)(|\uparrow\rangle+|\downarrow\rangle)(|\uparrow\rangle+|\downarrow\rangle)\\
&\xrightarrow{P_1=1} \frac{1}{2\sqrt{2}}(|\uparrow\uparrow\rangle+|\downarrow\downarrow\rangle)(|\uparrow\rangle+|\downarrow\rangle)(|\uparrow\rangle+|\downarrow\rangle)\\
&\xrightarrow{H} \frac{1}{4}(|\uparrow\uparrow\rangle+|\downarrow\uparrow\rangle+|\uparrow\downarrow\rangle-|\downarrow\downarrow\rangle)(|\uparrow\rangle+|\downarrow\rangle)(|\uparrow\rangle+|\downarrow\rangle)\\
&\xrightarrow{P_2=1} \frac{1}{2\sqrt{2}}(|\uparrow\uparrow\uparrow\rangle+|\downarrow\uparrow\uparrow\rangle+|\uparrow\downarrow\downarrow\rangle-|\downarrow\downarrow\downarrow\rangle)(|\uparrow\rangle+|\downarrow\rangle)\\
&\xrightarrow{H,H} \frac{1}{2\sqrt{2}}(|\uparrow\uparrow\uparrow\rangle+|\uparrow\downarrow\downarrow\rangle+|\downarrow\uparrow\downarrow\rangle+|\downarrow\downarrow\uparrow\rangle)(|\uparrow\rangle+|\downarrow\rangle)\\
&\xrightarrow{P_3=0} \frac{1}{2}(|\uparrow\uparrow\uparrow\downarrow\rangle+|\uparrow\downarrow\downarrow\uparrow\rangle+|\downarrow\uparrow\downarrow\uparrow\rangle+|\downarrow\downarrow\uparrow\uparrow\rangle)\\
&\xrightarrow{\sigma_x^4} |\chi\rangle. \qquad (9)
\end{aligned}$$

The other measurement results and the corresponding local single-qubit rotations are listed in Table 3.

Table 3. The obtained output states and the single-qubit local rotation operations required for achieving the four-electron $|\chi\rangle$ state corresponding to different measurement values of charge detectors P_1, P_2, and P_3. Here σ_x^j and σ_z^i are Pauli operators on the spin qubit, and I is the identity operator.

P_1	P_2	P_3	Output state	Operations
1	1	1	$\frac{1}{2}(\|\uparrow\uparrow\uparrow\uparrow\rangle+\|\uparrow\downarrow\downarrow\downarrow\rangle+\|\downarrow\uparrow\downarrow\downarrow\rangle+\|\downarrow\downarrow\uparrow\uparrow\rangle)$	I
1	1	0	$\frac{1}{2}(\|\uparrow\uparrow\uparrow\downarrow\rangle+\|\uparrow\downarrow\downarrow\uparrow\rangle+\|\downarrow\uparrow\downarrow\uparrow\rangle+\|\downarrow\downarrow\uparrow\downarrow\rangle)$	σ_x^4
1	0	1	$\frac{1}{2}(\|\uparrow\uparrow\uparrow\uparrow\rangle-\|\uparrow\downarrow\downarrow\downarrow\rangle-\|\downarrow\uparrow\downarrow\downarrow\rangle+\|\downarrow\downarrow\uparrow\uparrow\rangle)$	$\sigma_z^1\otimes\sigma_z^2$
1	0	1	$\frac{1}{2}(\|\uparrow\uparrow\uparrow\downarrow\rangle-\|\uparrow\downarrow\downarrow\uparrow\rangle-\|\downarrow\uparrow\downarrow\uparrow\rangle+\|\downarrow\downarrow\uparrow\downarrow\rangle)$	$\sigma_z^1\otimes\sigma_z^2\otimes\sigma_x^4$
0	1	1	$\frac{1}{2}(\|\uparrow\uparrow\uparrow\uparrow\rangle+\|\uparrow\downarrow\downarrow\downarrow\rangle-\|\downarrow\uparrow\downarrow\downarrow\rangle-\|\downarrow\downarrow\uparrow\uparrow\rangle)$	$\sigma_z^2\otimes\sigma_z^3$
0	1	0	$\frac{1}{2}(\|\uparrow\uparrow\uparrow\downarrow\rangle+\|\uparrow\downarrow\downarrow\uparrow\rangle-\|\downarrow\uparrow\downarrow\uparrow\rangle-\|\downarrow\downarrow\uparrow\downarrow\rangle)$	$\sigma_z^2\otimes\sigma_z^3\otimes\sigma_x^4$
0	0	1	$\frac{1}{2}(\|\uparrow\uparrow\uparrow\uparrow\rangle-\|\uparrow\downarrow\downarrow\downarrow\rangle+\|\downarrow\uparrow\downarrow\downarrow\rangle-\|\downarrow\downarrow\uparrow\uparrow\rangle)$	σ_z^2
0	0	0	$\frac{1}{2}(\|\uparrow\uparrow\uparrow\downarrow\rangle-\|\uparrow\downarrow\downarrow\uparrow\rangle+\|\downarrow\uparrow\downarrow\uparrow\rangle-\|\downarrow\downarrow\uparrow\downarrow\rangle)$	$\sigma_z^2\otimes\sigma_x^4$

3.3. Four-electron symmetric Dicke state

The Dicke state is an important multi-particle entangled state, and represents a particularly interesting set of quantum states associated with high robustness against particle loss and nonlocal properties of genuine entangled states.[54–56] We propose a network for the preparation of a novel four-electron entangled state $|D_4^{(2)}\rangle$ based on the CNOT gate in Ref. [23] as shown in Fig. 5, which can be written as

$$|D_4^{(2)}\rangle = \frac{1}{\sqrt{6}}(|\uparrow\uparrow\downarrow\downarrow\rangle+|\uparrow\downarrow\uparrow\downarrow\rangle+|\downarrow\uparrow\uparrow\downarrow\rangle + |\uparrow\downarrow\downarrow\uparrow\rangle+|\downarrow\uparrow\downarrow\uparrow\rangle+|\downarrow\downarrow\uparrow\uparrow\rangle). \quad (10)$$

This state with two excitations is symmetric under all permutations of the qubits.

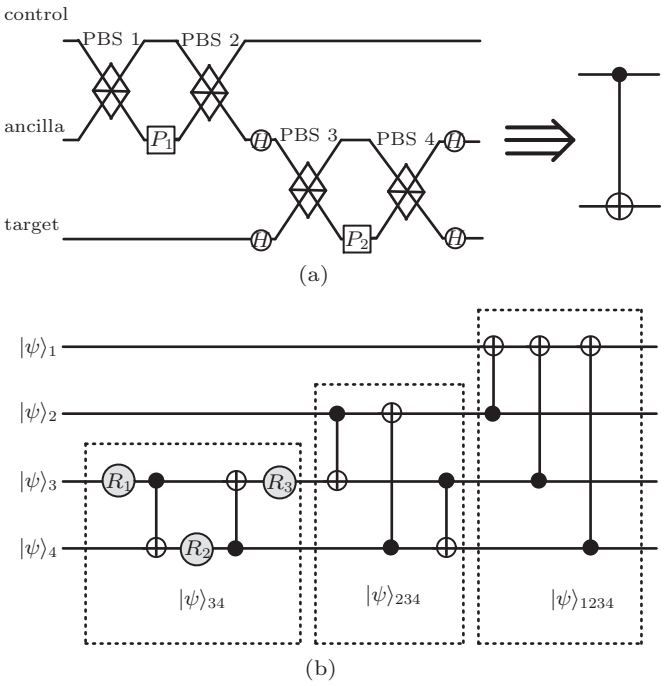


Fig. 5. The quantum circuit (a) for generating state $|D_4^{(2)}\rangle$ based on the CNOT gate proposed in Ref. [23] (b), where R_i $(i=1,2,3)$ is a single-qubit rotation.

The R_i $(i=1,2,3)$ is a single-qubit rotation defined by

$$R_i(\theta)|\uparrow\rangle = \cos\theta|\uparrow\rangle+\sin\theta|\downarrow\rangle,$$

$$R_i(\theta)|\downarrow\rangle = -\sin\theta|\uparrow\rangle+\cos\theta|\downarrow\rangle. \quad (11)$$

As shown in Fig. 5, electrons 1, 3, and 4 are prepared in state $|\uparrow\rangle$, and electron 2 is prepared in state $(|\uparrow\rangle+|\downarrow\rangle)/\sqrt{2}$. After the first part of the circuit, the state $|\Psi\rangle_{34}$ is constructed as

$$\begin{aligned}|\Psi\rangle_{34} &= R_3(\theta_3)C_{43}R_2(\theta_2)C_{34}R_1(\theta_1)|\uparrow\uparrow\rangle_{34}\\ &= \frac{1}{\sqrt{3}}(|\uparrow\downarrow\rangle+|\downarrow\uparrow\rangle+|\downarrow\downarrow\rangle),\end{aligned} \quad (12)$$

where C_{xy} is a CNOT gate with x as the controlling qubit and y as the target qubit, and $\theta_1=\theta_3=\arcsin\sqrt{1/2+\sqrt{5}/10}$ and $\theta_2=-\arcsin\sqrt{1/2+\sqrt{5}/6}$ have been chosen. After the second part, we obtain the following state:

$$\begin{aligned}|\Psi\rangle_{234} &= C_{34}C_{42}C_{23}|\Psi\rangle_2|\Psi\rangle_{34}\\ &= \frac{1}{\sqrt{6}}(|\uparrow\downarrow\uparrow\rangle+|\downarrow\uparrow\uparrow\rangle+|\uparrow\uparrow\downarrow\rangle\\ &\quad +|\downarrow\uparrow\downarrow\rangle+|\uparrow\downarrow\downarrow\rangle+|\downarrow\downarrow\uparrow\rangle).\end{aligned} \quad (13)$$

After the third part, we obtain

$$\begin{aligned}|D_4^{(2)}\rangle &= |\Psi\rangle_{1234}=C_{41}C_{31}C_{21}|\Psi\rangle_1|\Psi\rangle_{234}\\ &= \frac{1}{\sqrt{6}}(|\downarrow\uparrow\downarrow\uparrow\rangle+|\downarrow\downarrow\uparrow\uparrow\rangle+|\downarrow\uparrow\uparrow\downarrow\rangle\\ &\quad +|\uparrow\downarrow\uparrow\downarrow\rangle+|\uparrow\uparrow\downarrow\downarrow\rangle+|\uparrow\downarrow\downarrow\uparrow\rangle).\end{aligned} \quad (14)$$

The success probability of obtaining the symmetric Dicke state in our present scheme is 100%, which exceeds the probability of 3/8 obtained by applying the cross-Kerr nonlinearity in Ref. [57].

4. Discussion and summary

Charge detection has been realized by means of point contacts in a two-dimensional electron gas and using a quantum dot with a resonant conductance.[58–63] For instance, Field *et al.* used the effect of the electric field of the charge on the conductance of an adjacent point contact to realize charge detection in 1993.[59] Elzerma *et al.* reported their experimental results that the current achievable time resolution for charge detection is μs in 2004.[60] Their realization of such a device can be seen as a specific example of the general class of mesoscopic quadratic quantum measurement detectors.[61] The mesoscopic electron BS used in the present scheme can be realized by using a lithographically patterned metallic split gate[62] or by applying a small bias voltage to tune the splitting ratio.[63] In the charge detection process, the qubit interacts with a detector, and no qubit–qubit interaction occurs, so the detection is nondestructive. In addition, the success probabilities of the present schemes can reach unity under ideal conditions.

In summary, we have proposed schemes for implementing the HBSA and generate three kinds of four-electron high

entangled states based on charge detection of free electrons. The present schemes do not need an auxiliary system because the charge detection does not require interaction between the qubits. The HBSA and the generation of high entangled states with free electrons provide a promising way forward for quantum information processing.

References

[1] Bennett C H, Brassard G, Crepeau C, Jozsa R, Peres A and Wootters W K 1993 *Phys. Rev. Lett.* **70** 1895
[2] Ekert A K 1991 *Phys. Rev. Lett.* **67** 661
[3] Bennett C H, Brassard G and Mermin N D 1992 *Phys. Rev. Lett.* **68** 557
[4] Hillery M, Buăek V and Berthiaume A 1999 *Phys. Rev. A* **59** 1829
[5] Xiao L, Long G L, Deng F G and Pan J W 2004 *Phys. Rev. A* **69** 052307
[6] Yan F L and Gao T 2005 *Phys. Rev. A* **72** 012304
[7] Gu B, Mu L L, Ding L G, Zhang C Y and Li C Q 2010 *Opt. Commun.* **283** 3099
[8] Bennett C H, Brassard G and Mermin N D 1992 *Phys. Rev. Lett.* **68** 557
[9] Li X H, Deng F G and Zhou H Y 2008 *Phys. Rev. A* **78** 022321
[10] Zhou Y Y, Zhou X J, Tian P G and Wang Y J 2013 *Chin. Phys. B* **22** 010305
[11] Ekert A K 1991 *Phys. Rev. Lett.* **67** 661
[12] Man Z X, Zhang Z J and Li Y 2005 *Chin. Phys. Lett.* **22** 18
[13] Li X H, Deng F G and Zhou H Y 2006 *Phys. Rev. A* **74** 054302
[14] Zhu A D, Xia Y, Fan Q B and Zhang S 2006 *Phys. Rev. A* **73** 022338
[15] Long G L and Liu X S 2002 *Phys. Rev. A* **65** 032302
[16] Deng F G, Long G L and Liu X S 2003 *Phys. Rev. A* **68** 042317
[17] Deng F G and Long G L 2004 *Phys. Rev. A* **69** 052319
[18] Wang C, Deng F G, Li Y S, Liu X S and Long G L 2005 *Phys. Rev. A* **71** 044305
[19] Gu B, Huang Y G, Fang X and Chen Y L 2011 *Commun. Theor. Phys.* **56** 659
[20] Gu B, Huang Y G, Fang X and Zhang C Y 2011 *Chin. Phys. B* **20** 100309
[21] Gu B, Zhang C Y, Cheng G S and Huang Y G 2011 *Sci. China: Phys. Mech. Astron. B* **54** 942
[22] Zhang X L, Feng M and Gao K L 2006 *Phys. Rev. A* **73** 014301
[23] Tang L 2009 *Chin. Phys. B* **18** 1674
[24] Yu T, Zhu A D and Zhang S 2011 *Phys. Scr.* **84** 025001
[25] Briegel H J and Raussendorf R 2001 *Phys. Rev. Lett.* **86** 910
[26] Zhang G, Zhou J and Xue Z Y 2013 *Chin. Phys. B* **22** 040307
[27] Su S L, Wang Y, Guo Q, Wang H F and Zhang S 2012 *Chin. Phys. B* **21** 044205
[28] Gottesman D and Chuang I L 1999 *Nature* **402** 390
[29] Kiesel N, Schmid C, Tóth G, Solano E and Weinfurter H 2007 *Phys. Rev. Lett.* **98** 063604
[30] Rausendorf R and Briegel H J 2001 *Phys. Rev. Lett.* **86** 5188
[31] Kwiat P G and Weinfurter H 1998 *Phys. Rev. A* **58** 2623
[32] Walborn S P, Pádua S and Monken C H 2003 *Phys. Rev. A* **68** 042313
[33] Sheng Y B, Deng F G and Long G L 2010 *Phys. Rev. A* **82** 032318
[34] Ren B C, Wei H R, Hua M, Li T and Deng F G 2012 *Opt. Express* **20** 24664
[35] Ren B C, Wei H R and Deng F G 2013 *Laser Phys. Lett.* **10** 095202
[36] Wang T J, Lu Y and Long G L 2012 *Phys. Rev. A* **86** 042337
[37] Simon C and Pan J W 2002 *Phys. Rev. Lett.* **89** 257901
[38] Sheng Y B, Deng F G and Zhou H Y 2008 *Phys. Rev. A* **77** 042308
[39] Sheng Y B and Deng F G 2010 *Phys. Rev. A* **81** 032307
[40] Sheng Y B and Deng F G 2010 *Phys. Rev. A* **82** 044305
[41] Li X H 2010 *Phys. Rev. A* **82** 044304
[42] Deng F G 2011 *Phys. Rev. A* **83** 062316
[43] Sheng Y B, Long G L and Deng F G 2012 *Phys. Lett. A* **376** 314
[44] Wang T J, Song S Y and Long G L 2012 *Phys. Rev. A* **85** 062311
[45] Engel H A and Loss D 2005 *Science* **309** 586
[46] Beenakker C W J, DiVincenzo D P, Emary C and Kindermann M 2004 *Phys. Rev. Lett.* **93** 020501
[47] Feng X L, Kwek L C and Oh C H 2005 *Phys. Rev. A* **71** 064301
[48] Sheng Y B, Deng F G and Zhou H Y 2009 *Phys. Lett. A* **373** 1823
[49] Sheng Y B, Deng F G and Long G L 2011 *Phys. Lett. A* **375** 396
[50] Wang H F, zhang S and Zhu A D 2012 *Chin. Phys. B* **21** 040306
[51] Zhou L 2013 *Quantum Information Processing* **12** 2087
[52] Ionicioiu R 2007 *Phys. Rev. A* **75** 032339
[53] Wu C F, Yeo Y, Kwek L C and Oh C H 2007 *Phys. Rev. A* **75** 032332
[54] Stockton J K, Geremia J M, Doherty A C and Mabuchi H 2003 *Phys. Rev. A* **67** 022112
[55] Usha Devi A R, Prabhu R and Rajagopal A K 2007 *Phys. Rev. A* **76** 012322
[56] Retzker A, Solano E and Reznik B 2007 *Phys. Rev. A* **75** 022312
[57] Zhao C R and Ye L 2011 *Opt. Commun.* **284** 541
[58] Buks E, Schuster R, Heiblum M, Mahalu D and Umansky V 1998 *Nature* **391** 871
[59] Field M, Smith C G, Pepper M, Ritchie D A, Frost J E F, Jones G A C and Hasko D G 1993 *Phys. Rev. Lett.* **70** 1311
[60] Elzerman J M, Hanson R, Willems van Beveren L H, Vandersypen L M K and Kouwenhoven LP 2004 *Appl. Phys. Lett.* **84** 4617
[61] Mao W, Averin D V, Ruskov R and Korotkov A N 2004 *Phys. Rev. Lett.* **93** 056803
[62] Henny M, Oberholzer S, Strunk C, Heinzel T, Ensslin K, Holland M and Schönenberger C 1999 *Science* **284** 296
[63] Oliver W D, Kim J, Liu R C and Yamamoto Y 1999 *Science* **284** 299